JOURNAL OF CATALYSIS **171,** 449–456 (1997)
ARTICLE NO. CA971810

Location of Active Sites for 3-Pentanone Formation during Ethene Hydroformylation on Rh/Active-Carbon Catalysts

Hirotoshi Sakagami, Naoki Ohta, Shunsuke Endo, Teruyuki Harada, Nobuo Takahashi,[1]
and Takeshi Matsuda

Department of Materials Science, Kitami Institute of Technology, 165 Koencho, Kitami, Hokkaido 090, Japan

Received February 10, 1997; revised June 24, 1997; accepted June 24, 1997

In ethene hydroformylation over Rh/active carbon prepared from $RhCl_3$, 3-pentanone was formed in addition to propanal, which was a common product in the reaction. In the case of propene hydroformylation, however, butanal was exclusively formed and no appreciable formation of ketones was observed. On the catalyst treated with CO at 473 K, both activities for propanal and butanal formation were observed to be higher than those on the catalyst untreated. An approximate linear relation between the activity for propanal formation and that for butanal formation was observed, indicating that the active sites for aldehyde formation can catalyze the reaction for both ethene and propene. On the other hand, the activity for 3-pentanone formation was reduced by the CO treatment. These results indicate that the transformation of active species for 3-pentanone formation into the active species for aldehyde formation was induced by the CO treatment. On the catalyst treated with CO, a value for *n*/iso- ratio in butanal formed was observed to be higher than that on the catalyst untreated. These results suggest the formation of new active Rh particles in the narrower pores. On the basis of the results obtained, the active species for 3-pentanone formation was thought to be located in the narrow pores, where the formation of reaction intermediates of C_7-ketones from propene would be strongly suppressed because of their bulky structure compared with that for 3-pentanone. © 1997 Academic Press

INTRODUCTION

Rhodium supported on active carbon can catalyze ethene hydroformylation as well as other supported rhodium catalysts (1–4). In the reaction over the former catalyst, however, 3-pentanone is formed in addition to propanal, which is a common hydroformylation product from ethene. The following results were obtained in the previous work: (i) an increase in the temperature for the pretreatment of the catalyst with H_2 reduced the activity for 3-pentanone formation (denoted by $r_{3\text{-P}}$), while the activity for propanal formation (denoted by r_{PA}) was enhanced; (ii) although $r_{3\text{-P}}$ rapidly decreased with time on stream at reaction temperatures >413 K, r_{PA} slowly decreased even at 453 K; (iii) r_{PA} decreased with an increase in CO partial pressure, while $r_{3\text{-P}}$ increased; (iv) $r_{3\text{-P}}$ decreased when the catalyst was exposed to CO at >433 K, whereas r_{PA} was enhanced by this treatment; and (v) the active sites for 3-pentanone formation required the presence of chlorine to be formed but those for propanal formation did not. These results indicate that the active sites for 3-pentanone formation are different from those for propanal formation. It was already reported that the propanal formation is accelerated by the presence of rhodium metal particles (5, 6). Chuang *et al.* have proposed Rh^+ sites at the surface of supported rhodium metal particles as the active sites for the propanal formation on Rh/SiO_2 (7–9). The Rh/active-carbon catalyst which showed high activity for 3-pentanone formation adsorbed a considerable amount of CO, and it showed a CO desorption peak at almost the same position with $Rh_6(CO)_{16}$-like species formed on Y-zeolite (10). In addition, EXAFS analysis of this sample suggested the presence of $Rh_6(CO)_{16}$-like species (11). On the basis of the results obtained, we suggested an important role of the Rh–CO species in forming the active species for 3-pentanone formation.

Formation of C_7-ketones was reported by Rode *et al.* in propene hydroformylation over Rh supported Y-zeolite catalysts (12). If the Rh/active carbon could catalyze propene hydroformylation, *n*-butanal and isobutanal would be formed. In addition, three kinds of ketones (4-heptanone, 2-methyl-3-hexanone, and 2,4-dimethyl-3-pentanone) are expected to be produced. Active carbon is one of the typical microporous materials. If the active sites for ketone formation were located in the narrow pores, a ratio of (ketone)/(aldehyde) would be small in propene hydroformylation compared with that in ethene hydroformylation, since the intermediates of ketones are more bulky than those for aldehydes. The ratio of (*n*-butanal)/(isobutanal) may also reflect the location of active sites for aldehyde formation, since the intermediate of isobutanal is more bulky than that for *n*-butanal. In the present work, the catalytic behavior of Rh/active carbon for propene hydroformylation has been compared with that for ethene

---

[1] To whom correspondence should be addressed.

0021-9517/97 $25.00
Copyright © 1997 by Academic Press
All rights of reproduction in any form reserved.

hydroformylation in order to clarify the location of active sites for 3-pentanone formation.

EXPERIMENTAL

The active-carbon support (obtained from Wako Pure Chemical Ind., Ltd., specific surface area 930 m^2/g, average pore diameter (d_{av}) 4 nm) was washed with 0.1 mol/dm^3 of hydrochloric acid solution and thoroughly washed with deionized water. Rh/active carbon with 2.0 wt% Rh loading was prepared by a conventional impregnation method, where rhodium trichloride trihydrate ($RhCl_3 \cdot 3H_2O$) or rhodium trinitrate ($Rh(NO_3)_3$) was deposited on the support from the aqueous solution of them. The solid was dried at 383 K for 12 h in an oven. In the same manner, Rh/molecular sieve carbon 3 Å ($d_{av} < 0.5$ nm, obtained from Takeda Chemical Industries, Ltd.) was prepared. Rh/SiO_2 catalysts were prepared in the same manner by using SiO_2 with different pore sizes (A, obtained from Nishio Industry Co., Ltd.; B–D, obtained from Fuji Sylicia Chemical Ind. as CARIACT Nos. 10, 15, 30, and 50, respectively). Values for average pore diameter of SiO_2 used were measured by Carlo Erba Sorptmatic 1900.

Pretreatment of the catalyst with H_2 at 573 K for 3 h was followed by ethene or propene hydroformylation at 393 K with a reactant gas mixture of He–C_2H_4(or C_3H_6)(20%)–CO(20%)–H_2(20%) (total flow rate 100 cm^3(STP)/min) in a fixed-bed type reactor with a continuous flow operated at atmospheric pressure. If necessary, the pretreatment with H_2 was followed by a treatment with CO at 473 K for 1 h prior to the reaction performance.

The amounts of H_2 or CO adsorbed on the catalyst were measured at 296 K by a conventional static method using a glass-made apparatus connected to a vacuum line. For the estimation of the amount of H_2 or CO required for a monolayer coverage of a Rh metal surface, we used a single H_2 or CO isotherm. Namely, the value for the monolayer coverage was estimated by extrapolating the flat part of an adsorption isotherm to the zero of the equilibrium pressure for adsorption. The amounts of H_2 and CO adsorbed on the active carbon support itself ($<1 \times 10^{-6}$ mol g-cat^{-1}) were found to be much less than those on the Rh/active-carbon catalysts. Assuming that each surface rhodium atom can adsorb one H atom or one CO molecule, the dispersion of rhodium was evaluated from the value for the monolayer coverage.

Transmission electron micrographs of the samples were obtained by using a JEOL JEM-2010F electron microscope with an energy dispersive X-ray spectrometer (EDS) in cooperation with JEOL Ltd. (at 200 kV and direct magnification of 400,000). Samples were exposed to air and crushed into fine particles for the measurements by TEM.

RESULTS AND DISCUSSION

In ethene hydroformylation over Rh/active carbon (denoted by Rh/AC), propanal, 3-pentanone, and ethane were formed (1–4). For the evaluation of the catalytic activity, we tried to determine the number of surface rhodium atoms on the catalysts by using H_2 or CO chemisorption technique. The amounts of H_2 and CO adsorbed on the rhodium catalysts prepared are shown in Table 1. In the case of SiO_2 support, the values for the ratio of the amount of CO to that of H_2 were observed to be around 2.0, suggesting that the normal adsorption of H_2 and CO to surface rhodium atoms (each surface rhodium atom can adsorb one H atom or one CO molecule) is predominant on the Rh/SiO_2 catalysts. On the other hand, the values of CO/H_2 were observed to be much higher than 2.0 on the Rh/AC catalysts, particularly on the Rh(C)/AC prepared from $RhCl_3$. The excess amount

TABLE 1

Adsorption of Hydrogen and Carbon Monoxide on the Catalysts Used

Catalyst	Rh loading (wt%)	Rh loading (10^{-6} mol g-cat^{-1})	H_2 adsorbed (10^{-6} mol g-cat^{-1})	CO adsorbed (10^{-6} mol g-cat^{-1})	CO/H_2	Rh dispersion (%) H_2	Rh dispersion (%) CO
Rh(C)/AC	1.0	97	15.0	139.4	9.3	31	144
Rh(C)/AC	2.0	194	31.6	267.5	8.5	33	138
Rh(C)/AC	3.0	292	46.4	384.0	8.3	32	132
Rh(C)/AC	4.0	389	54.7	488.8	8.9	28	126
Rh(N)/AC	2.0	194	15.5	48.8	3.1	16	25
Rh(N)/AC	4.0	389	45.3	189.3	4.2	23	49
Rh/SiO_2(A)	4.0	389	66.9	141.8	2.1	34	36
Rh/SiO_2(B)	4.0	389	69.0	137.0	2.0	35	35
Rh/SiO_2(C)	4.0	389	53.0	90.9	1.7	27	23
Rh/SiO_2(D)	4.0	389	36.2	63.8	1.8	19	16
Rh/SiO_2(E)	4.0	389	28.8	54.4	1.9	15	14
Rh(C)/MSC	2.0	194	6.9	19.5	2.8	7	10

TABLE 2

Comparison of C_3H_6 Hydroformylation with C_2H_4 Hydroformylation over Rh/AC

Run	Catalyst	Rh loading (wt%)	Treatment with CO[a]	Reaction of C_2H_4 (TOF, 10^{-3} min^{-1})			Reaction of C_3H_6 (TOF, 10^{-3} min^{-1})				
				r_{PA}	$r_{3\text{-}P}$	r_E	$r_{n\text{-}BA}$	$r_{i\text{-}BA}$	r_{BA}[b]	r_P	*n*-BA/i-BA
1	Rh(C)/AC	1.0	No	32	19	67	11	10	21	66	1.1
2	Rh(C)/AC	1.0	Yes	252	6	265	80	48	128	186	1.7
3	Rh(C)/AC	2.0	No	66	9	114	16	13	28	55	1.2
4	Rh(C)/AC	2.0	Yes	357	5	376	102	59	160	172	1.7
5	Rh(C)/AC	3.0	No	87	5	147	19	14	33	52	1.3
6	Rh(C)/AC	3.0	Yes	383	3	405	115	65	180	175	1.8
7	Rh(C)/AC	4.0	No	100	3	142	26	18	44	52	1.4
8	Rh(C)/AC	4.0	Yes	407	2	311	116	63	178	127	1.8
9	Rh(N)/AC	2.0	No	85	0	114	15	10	25	60	1.5
10	Rh(N)/AC	2.0	Yes	80	0	107	15	10	25	59	1.5
11	Rh(N)/AC	4.0	No	113	1	139	25	16	41	50	1.6
12	Rh(N)/AC	4.0	Yes	132	0	139	36	21	57	63	1.7

Note. Catalytic activities, rates of formation at time-on-stream of 8 h.

[a] Pretreatment of the catalyst with H_2 was followed by the treatment with CO at 473 K for 1 h.

[b] $r_{BA} = r_{n\text{-}BA} + r_{i\text{-}BA}$.

of CO adsorbed over Rh atoms on the Rh/AC catalysts was already observed by means of a temperature-programmed desorption technique (TPD) (3, 4, 11). The higher values of CO/H_2 indicate the presence of highly dispersed phase of Rh. In the present work, the number of surface rhodium atoms was evaluated by using the amount of H_2 required for the molayer coverage.

In the ethene hydroformylation at 393 K, the rates of propanal and ethane formation slowly decreased with time on stream. The rate of 3-pentanone formation, on the other hand, increased with time on stream at the early stage of the reaction for about 8 h, and then it decreased slowly. As shown in Fig. 1, *n*-butanal, isobutanal, and propane were observed to be the products in propene hydroformylation over Rh(C)/AC (2.0 wt%). The rates for the formation of the three products are denoted by $r_{n\text{-}BA}$, $r_{i\text{-}BA}$, and r_P, respectively. However, no appreciable formation of C_7-ketones was observed. In the present work, the catalytic activities are evaluated by the rates of formation at time on stream of 8 h.

In Table 2, the catalytic behaviors of Rh/AC for propene hydroformylation are compared with those for ethene hydroformylation. On both Rh/AC catalysts, Rh(C)/AC and Rh(N)/AC (prepared from $Rh(NO_3)_3$), the activity for butanal formation ($r_{BA} = r_{n\text{-}BA} + r_{i\text{-}BA}$) in propene hydroformylation increased with an increase in the amount of Rh loaded. An approximate linear relation was observed between r_{BA} and r_{PA} as shown by open circles for Rh(C)/AC and open squares for Rh(N)/AC in Fig. 2. Namely, the active sites for aldehyde formation can catalyze the reaction

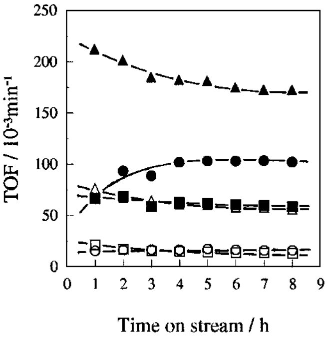

FIG. 1. Propene hydroformylation over Rh(C)/AC (2 wt%) with H_2 pretreatment at 573 K (○, □, △) and with CO treatment at 473 K after the H_2 treatment (●, ■, ▲). (○, ●, *n*-butanal; □, ■, isobutanal; △, ▲, propane).

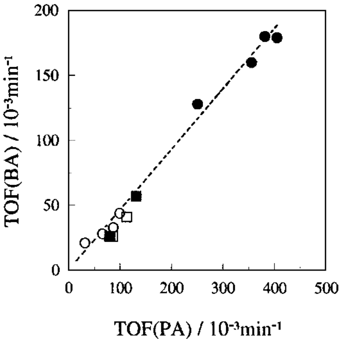

FIG. 2. Plots for r_{PA} vs r_{BA} on Rh(C)/AC (○, ●) and on Rh(N)/AC (□, ■). (○ and □, with H_2 pretreatment at 573 K; ● and ■, with CO treatment at 473 K after the H_2 treatment).

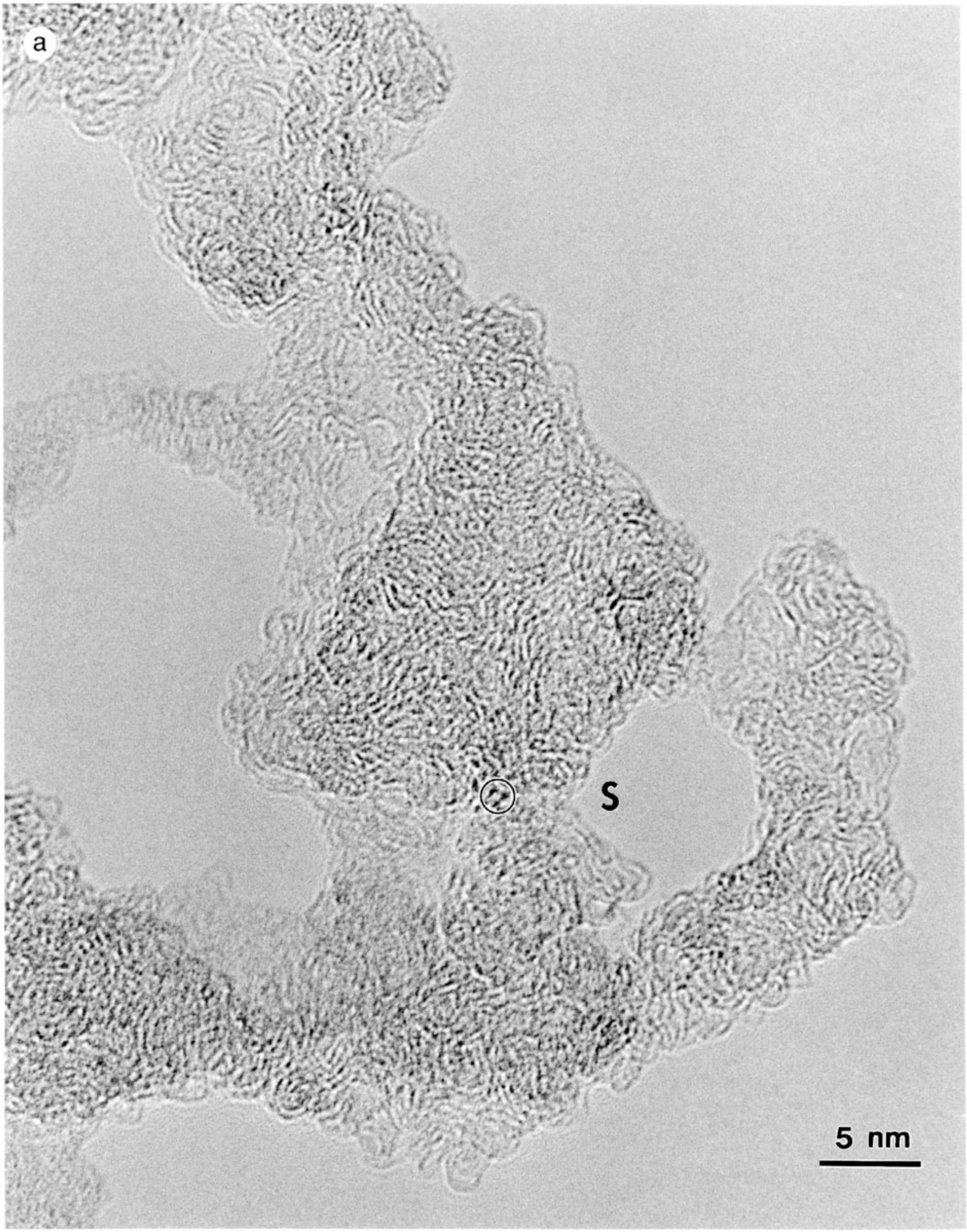

FIG. 3. (a) A TEM photograph on Rh(C)/AC (2 wt%) with H_2 pretreatment at 573 K; (b) an energy-dispersive X-ray spectrum on the spot shown in (a).

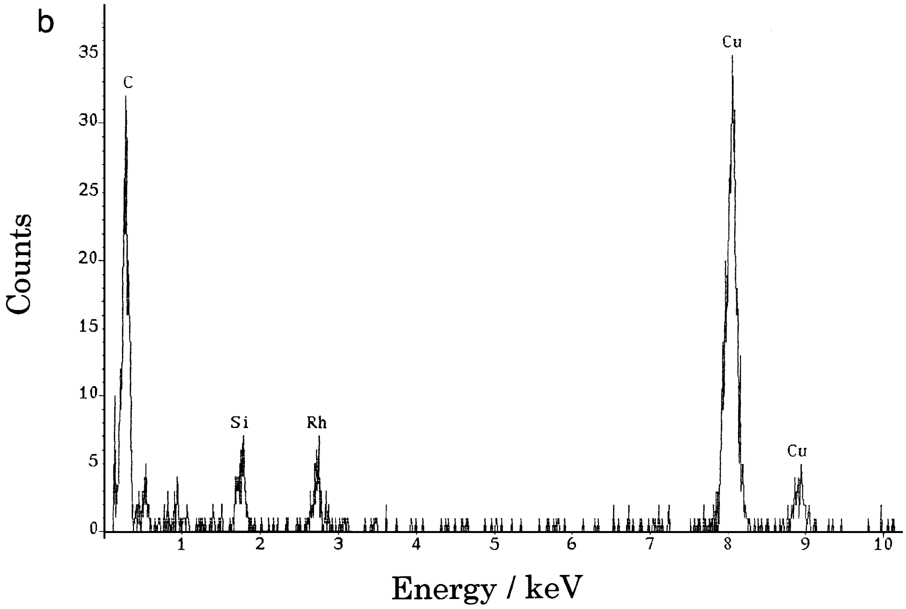

FIG. 3—*Continued*

for both of olefins, ethene, and propene. In the case of Rh(N)/AC, $r_{3\text{-P}}$ was observed to be very low as previously reported (4). On both catalysts, Rh(C)/AC and Rh(N)/AC, formation of C_7-ketones from C_3H_6 could not be observed. After the reaction over Rh(C)/AC with propene, olefin in the reaction gas mixture was replaced from propene to ethene. In this case, formation of 3-pentanone was observed, indicating that the active sites for 3-pentanone formation kept their activity during the reaction with propene. Thus, the active sites for 3-pentanone formation could not contribute to the C_7-ketone formation from propene.

We have previously reported that r_{PA} on the catalyst prepared from $RhCl_3$ was enhanced by the treatment of the catalyst with CO at temperatures >433 K, while $r_{3\text{-P}}$ was reduced (3, 4). The effect of the CO treatment were confirmed on Rh(C)/AC as shown in Table 2. In propene hydroformylation, r_{BA} was also enhanced by the CO treatment of Rh(C)/AC, as typically shown in Fig. 1 on the catalyst with 2.0 wt% Rh. No important effects of the treatment with CO, however, were observed both on r_{PA} and on r_{BA} in the case of Rh(N)/AC. The plots of r_{PA} vs r_{BA} on the catalysts with the CO treatment are shown by filled circles for Rh(C)/AC and filled squares for Rh(N)/AC in Fig. 2. They fall on almost the same line for the catalysts without the CO treatment. This indicates that the active sites for propanal formation, which are newly formed by the CO treatment, can catalyze butanal formation. The newly formed active sites would be formed from the Rh–CO species, which were responsible for 3-pentanone formation. The transformation of the fine Rh aggregates into Rh metal particles, which was induced by the CO treatment at higher temperatures than 423 K, was reported in several cases of Rh/inorganic supports (13–19). We also suggested such structural changes of Rh on active-carbon support on the basis of the results by means of EXAFS and TPD techniques (11). In order to make this point more clear, we tried to observe the particle

TABLE 3

Effects of CO Treatment of Rh/AC at 473 K on H_2 and CO Adsorption

Catalyst	Rh loading (wt%)	Rh loading (10^{-6} mol g-cat^{-1})	H_2 adsorbed (10^{-6} mol g-cat^{-1})	CO adsorbed (10^{-6} mol g-cat^{-1})	CO/H_2	Rh dispersion (%) H_2	Rh dispersion (%) CO
Rh(C)/AC	1.0	97	7.5	35.5	4.7	15	37
Rh(C)/AC	2.0	194	13.7	64.3	4.7	14	33
Rh(C)/AC	3.0	292	19.2	113.1	5.9	13	39
Rh(C)/AC	4.0	389	22.9	134.5	5.9	12	35
Rh(N)/AC	2.0	194	15.5	51.5	3.3	16	27
Rh(N)/AC	4.0	389	34.4	109.8	3.2	18	28

FIG. 4. (a) A TEM photograph on Rh(C)/AC (2 wt%) with CO treatment at 473 K after the H_2 treatment; (b) an energy-dispersive X-ray spectrum on the spot shown in (a).

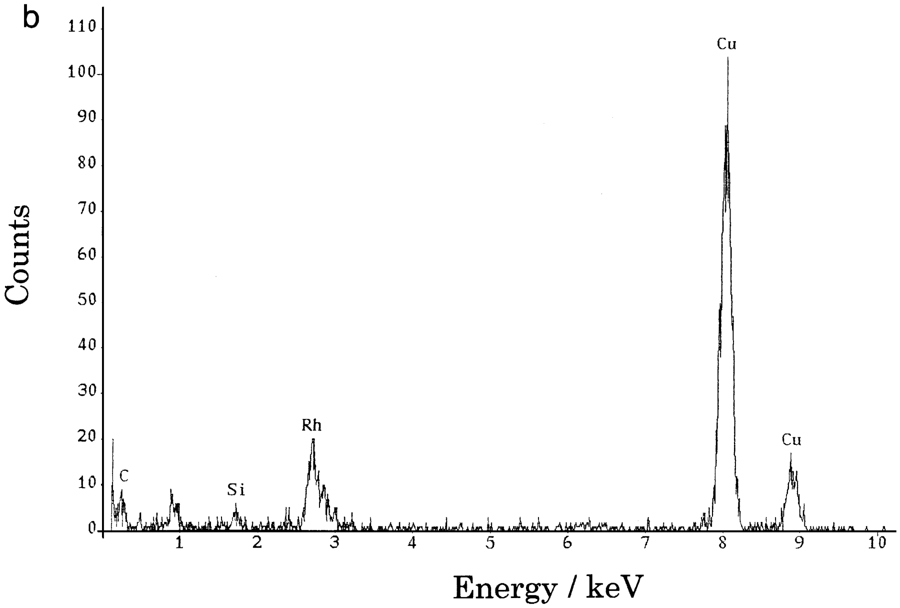

FIG. 4—*Continued*

sizes of rhodium on Rh(C)/AC both treated and untreated with CO by a transmission electron microscopy (TEM). A TEM photograph on the Rh(C)/AC treated with H_2 at 573 K is shown in Fig. 3a. No particles of Rh were observed, where EDS measurements showed that very small aggregates of Rh and/or cationic Rh species were present in the diffused phase, as typically shown in Fig. 3b. The result agrees with that by EXAFS where Rh–O bonds were predominantly observed (11). In the case of the Rh(C)/AC with the CO treatment at 473 K, on the other hand, the presence of fine Rh particles (ca. 2 nm) was clearly observed as shown by Figs. 4a and 4b. These results support that the transformation of the Rh–CO species into fine metal particles of Rh is responsible for the enhancement in r_{PA} and the reduction in $r_{\mathrm{3\text{-}P}}$. The effects of the CO treatment on the adsorption of H_2 and CO are shown in Table 3. The higher values of CO/H_2 ratio than 2.0 indicates the presence of the highly dispersed phase of Rh even after the CO treatment.

In contrast to the Rh/AC catalysts, no appreciable formation of 3-pentanone was observed during ethene hydroformylation over Rh/SiO_2. In propene hydroformylation over Rh/SiO_2, formation of butanal was observed, while formation of C_7-ketones was not. Typical time courses of the hydroformylation products over Rh/SiO_2(D) are compared with those over Rh/SiO_2(A) in Fig. 5. On the former ($d_{\mathrm{av}} = 30$ nm), $r_{\mathrm{i\text{-}BA}}$ was found to be much higher than $r_{n\text{-}\mathrm{BA}}$ (n/iso- = 0.4). On the latter ($d_{\mathrm{av}} = 6$ nm), $r_{\mathrm{i\text{-}BA}}$ was higher than $r_{n\text{-}\mathrm{BA}}$ at the initial stage of the reaction. However, $r_{\mathrm{i\text{-}BA}}$ decreased more rapidly than $r_{n\text{-}\mathrm{BA}}$, and $r_{n\text{-}\mathrm{BA}}$ exceeded $r_{\mathrm{i\text{-}BA}}$ after the time on stream of 2 h. The value for n/iso- ratio for butanal formed at time on stream of 8 h was found to be ca. 1.4. The results of propene hydroformylation over Rh/SiO_2 catalysts, prepared by using SiO_2 with different average pore diameters, are summarized in Table 4. The values for n/iso- ratio on SiO_2 with narrow pores (A and B) were observed to be higher than those on SiO_2 with wide pores (C, D, E). The values arround 0.4 on the latter are close to that on Rh(C)/molecular sieve carbon (denoted by MSC) as shown by run 6 in Table 4. In the case of MSC, the reaction took place on the active rhodium sites present at the external surface of MSC, since even C_2H_4 molecules could not enter the narrow pores of it. Thus, the propene hydroformylation over the active sites in the wide space is characterized by the lower n/iso- ratio in butanal formed. As shown in Table 2, the n/iso- ratios on the Rh/AC catalysts without the CO treatment were observed to be 1.1–1.4. The active sites for propanal formation on Rh/AC are located in the relatively narrow pores as in the case of SiO_2(A). As can be seen form Fig. 1 and Table 2, the n/iso- ratios were observed

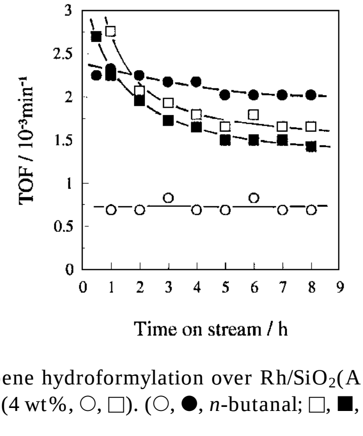

FIG. 5. Propene hydroformylation over Rh/SiO_2(A) (4 wt%, ●, ■) and Rh/SiO_2(D) (4 wt%, ○, □). (○, ●, n-butanal; □, ■, isobutanal).

TABLE 4

Comparison of C_3H_6 Hydroformylation with C_2H_4 Hydroformylation over Rh/SiO_2

Run	Support				Rh loading (wt%)	Reaction of C_2H_4 (TOF, 10^{-3} min^{-1})		Reaction of C_3H_6 (TOF, 10^{-3} min^{-1})				
		A[a] (m^2 g^{-1})	d_{av}[b] (nm)	d_{av}[c] (nm)		r_{PA}	r_E	$r_{n\text{-BA}}$	$r_{i\text{-BA}}$	r_{BA}[d]	r_P	n-BA/i-BA
1	SiO_2(A)	380	—	6	4.0	17.9	28.6	2.0	1.4	3.4	11.8	1.4
2	SiO_2(B)	300	10	9	4.0	21.6	37.9	1.5	1.6	3.1	11.0	0.9
3	SiO_2(C)	190	15	14	4.0	13.1	34.2	0.8	1.6	2.4	12.9	0.5
4	SiO_2(D)	100	30	40	4.0	8.8	26.5	0.7	1.6	2.3	16.5	0.4
5	SiO_2(E)	90	50	—	4.0	9.9	27.7	0.6	1.7	2.2	19.3	0.3
6	MSC[e]	—	—	—	2.0	3.0	7.1	0.3	0.6	0.9	6.2	0.5

Note. r, catalytic activities, rates of formation at time-on-stream of 8 h.

[a] BET surface area.

[b] Average pore diameter by mercury porosimetry from commercial catalog.

[c] Average pore diameter by N_2 adsorption–desorption method with Carlo Erba Sorptmatic 1900.

[d] $r_{BA} = r_{n\text{-BA}} + r_{i\text{-BA}}$.

[e] Average pore diameter is <0.5 nm (reported by Takeda Chemical Industries, Ltd.).

to be 1.7–1.8 in the case of Rh/AC with the CO treatment and these values were higher than that on the untreated Rh/AC. This is probably due to the formation of new active Rh particles in the narrower pores. It is noted that the origins of the newly formed active species are the active species for 3-pentanone formation. Therefore, the active species for 3-pentanone formation would be located in the narrow pores, where the formation of intermediates for ketones from C_3H_6 would be strongly suppressed because of their bulky structure.

Consequently, the following results have been obtained in the present work: (i) the formation of C_7-ketones could not be observed in propene hydroformylation, while butanal formation was catalyzed as well as propanal formation over Rh/AC catalysts; (ii) on the catalyst with the CO treatment at 473 K, the active sites for aldehyde formation showed a higher ratio for *n*/iso- in butanal compared with that on the untreated catalyst. On the basis of the results obtained, the location of the active sites for 3-pentanone formation during ethene hydroformylation is suggested to be in the narrow pores on the active carbon support.

REFERENCES

1. Takahashi, N., Arakawa, H., Kano, A., Fukagawa, Y., and Asao, K., *Chem. Lett.* 205 (1990).
2. Takahashi, N., Takeyama, T., Yanagibashi, T., and Takada, Y., *J. Catal.* **136**, 531 (1992).
3. Takahashi, N., Sato, Y., Uchiumi, T., and Ogawa, K., *Bull. Chem. Soc. Jpn.* **66**, 1273 (1993).
4. Takahashi, N., Takabatake, Y., Sakagami, H., Imizu, Y., Okazaki, N., and Tada, A., *J. Catal.* **159**, 491 (1996).
5. Takahashi, N., and Kobayashi, M., *J. Catal.* **85**, 89 (1984).
6. Takahashi, N., Mijin, A., Suematsu, H., Shinohara, S., and Matsuoka, H., *J. Catal.* **117**, 348 (1989).
7. Chuang, S. S. C., and Pien, S. J., *J. Catal.* **135**, 618 (1992).
8. Chuang, S. S. C., Srinivas, G., and Mukherjee, A., *J. Catal.* **139**, 490 (1993).
9. Srinivas, G., and Chuang, S. S. C., *J. Phys. Chem.* **98**, 3024 (1994).
10. Takahashi, N., Mijin, A., Ishikawa, T., Nebuka, K., and Suematsu, H., *J. Chem. Soc. Faraday Trans. 1* **83**, 2605 (1987).
11. Takahashi, N., Takeyama, T., Fujimoto, T., Fukuoka, A., and Ichikawa, M., *Chem. Lett.* 1441 (1992).
12. Rode, E., Davis, M. E., and Hanson, B. E., *J. Chem. Soc. Chem. Commun.* 716 (1985).
13. Solymosi, F., and Pasztor, M., *J. Phys. Chem.* **89**, 4789 (1985).
14. Zaki, M. I., Kunzman, G., Gates, B. C., and Knozinger, H., *J. Phys. Chem.* **91**, 1486 (1987).
15. Solymosi, F., and Knozinger, H., *J. Chem. Soc. Faraday Trans.* **86**, 389 (1990).
16. Buchanan, D. A., Hernandez, M. E., Solymosi, F., and White, J. M., *J. Catal.* **125**, 456 (1990).
17. Solymosi, F., and Bansagi, T., *J. Phys. Chem.* **97**, 10133 (1993).
18. Kraus, K. R., Schabes-Retchkiman, P., and Schmidt, L. D., *J. Catal.* **134**, 204 (1992).
19. Berko, A., Menesi, G., and Solymosi, F., *J. Phys. Chem.* **100**, 17732 (1996).